



Published in final edited form as:

*Oncogene*. 2015 July ; 34(28): 3651–3661. doi:10.1038/onc.2014.294.

## CSF1-ETS2 Induced microRNA in Myeloid Cells Promote Metastatic Tumor Growth

Haritha Mathsyaraja<sup>1,2</sup>, Katie Thies<sup>1,2</sup>, David A. Taffany<sup>1,2</sup>, Clayton Deighan<sup>5</sup>, Tom Liu<sup>2</sup>, Lianbo Yu<sup>8</sup>, Soledad A. Fernandez<sup>8</sup>, Charles Shapiro<sup>2,4</sup>, Jose Otero<sup>2,3</sup>, Cynthia Timmers<sup>2</sup>, Maryam B. Lustberg<sup>2,4</sup>, Jeffrey Chalmers<sup>2,5</sup>, Gustavo Leone<sup>2,6,7</sup>, and Michael C. Ostrowski<sup>1,2</sup>

<sup>1</sup>Department of Molecular and Cellular Biochemistry, The Ohio State University College of Medicine

<sup>2</sup>The Comprehensive Cancer Center, The Ohio State University

<sup>3</sup>Department of Pathology, Ohio State University College of Medicine

<sup>4</sup>Department of Internal Medicine, The Ohio State University College of Medicine

<sup>5</sup>Department of Chemical Engineering, The Ohio State University

<sup>6</sup>Department of Molecular Virology, Immunology & Medical Genetics, The Ohio State University College of Medicine

<sup>7</sup>Department of Molecular Genetics, The Ohio State University, Columbus, OH 43210

<sup>8</sup>Center for Biostatistics, Department of Biomedical Informatics, The Ohio State University, Columbus, OH 43210

### Abstract

Metastasis of solid tumors is associated with poor prognosis and bleak survival rates. Tumor infiltrating myeloid cells (TIMs) are known to promote metastasis but the mechanisms underlying their collaboration with tumor cells remain unknown. Here we report an oncogenic role for microRNA in driving M2 reprogramming in TIMs, characterized by the acquisition of pro-tumor and pro-angiogenic properties. The expression of miR-21, miR-29a, miR-142-3p and miR-223 increased in myeloid cells during tumor progression in mouse models of breast cancer and melanoma metastasis. Further, we show that these miRs are regulated by the CSF1-ETS2 pathway in macrophages. A loss of function approach utilizing selective depletion of the microRNA processing enzyme *Dicer* in mature myeloid cells blocks angiogenesis and metastatic tumor growth. Ectopic expression of miR-21 and miR-29a promotes angiogenesis and tumor cell proliferation through the down-regulation of anti-angiogenic genes such as *Col4a2*, *Spry1* and

Users may view, print, copy, and download text and data-mine the content in such documents, for the purposes of academic research, subject always to the full Conditions of use:[http://www.nature.com/authors/editorial\\_policies/license.html#terms](http://www.nature.com/authors/editorial_policies/license.html#terms)

**Correspondence to:** Michael C. Ostrowski Department of Molecular & Cellular Biochemistry Tumor Microenvironment Program The Ohio State University 598 Biomedical Research Tower 460 W. 12th Ave Columbus, OH 43210 Telephone: 614-688-3824 FAX: 614-688-4181 michael.ostrowski@osumc.edu.

**CONFLICT OF INTEREST** The authors declare no conflict of interest.

Supplementary Information accompanies this paper on the *Oncogene* website (<http://www.nature.com/onc>)

*Timp3* whereas knockdown of the miRs impedes these processes. miR-21 and miR-29a are expressed in *Csf1r*+ myeloid cells associated with human metastatic breast cancer and levels of these miRs in CD115+ non-classical monocytes correlates with metastatic tumor burden in patients. Taken together, our results suggest that miR-21 and miR-29a are essential for the pro-tumor functions of myeloid cells and the CSF1-ETS2 pathway upstream of the miRs serves as an attractive therapeutic target for the inhibition of M2 remodeling of macrophages during malignancy. In addition, miR-21 and miR-29a in circulating myeloid cells may potentially serve as biomarkers to measure therapeutic efficacy of targeted therapies for CSF1 signaling.

## Keywords

Solid tumor metastasis; microRNA; macrophages

## INTRODUCTION

Macrophage infiltration is associated with poor prognosis in several different types of cancer, including breast cancer and melanoma.<sup>1,2,3</sup> The umbrella term ‘tumor infiltrating myeloid cells’ (TIMs) is used to describe mature myeloid cells and macrophages found within the tumor microenvironment, though it is likely unique subsets of cells mediate different steps in malignant disease progression.<sup>4</sup> Myeloid cells are crucial for establishing the pre-metastatic niche and fostering metastatic tumor growth.<sup>5,6,7</sup> Mammary TIMs are known to produce several growth factors and molecules including MMP9 and VEGFA that aid metastasis.<sup>7,8</sup> Melanoma associated myeloid cells also secrete factors such as CCL2, MMP9, Adrenomedullin and IFN- $\gamma$  that promote tumor cell invasiveness and enhance melanomagenesis.<sup>9,10,11</sup> Despite the growing body of evidence implicating TIMs in malignant disease progression, the mechanisms by which they remodel the distal metastatic site remain poorly defined. In addition, pathways that are activated in TIMs in response to cues from the metastatic tumor microenvironment that enable tumor establishment and growth are yet to be delineated.

The microRNAs (miRs) are small non-coding RNAs that act as powerful post-transcriptional regulators of cellular functions whose activities are frequently deranged in tumor cells.<sup>12</sup> Recent reports highlight the critical role that microRNA play in regulating inflammatory responses and macrophage polarization.<sup>13,14</sup> In the context of breast cancer, miR-155 and miR-511-3p expression in TIMs elicit tumor suppressive properties, leading to the inhibition of primary tumor growth.<sup>15,16</sup>

In the current study, evidence for a CSF1-ETS2 pathway driven oncogenic microRNA expression signature that includes miR-21 and miR-29a is presented. These oncogenic miRs function in metastasis-associated myeloid cells to promote tumor proliferation and angiogenesis. Further, our findings suggest that the oncogenic miRs are necessary for metastasis as specific ablation of Dicer in mature myeloid cells retards metastatic tumor progression in mouse models of both metastatic breast cancer and melanoma. In addition, knockdown on miR-21 and mir-29a in macrophages impedes tumor cell proliferation.

Analysis of human metastatic breast cancer samples implicates miR-21 and miR-29a in patients with metastatic disease.

## RESULTS

### microRNAs are differentially expressed in myeloid cells during metastatic tumor progression in mouse models of melanoma and breast cancer

In order to identify microRNA that are regulated in metastatic TIMs, an experimental metastasis assay was designed to examine metastatic melanoma and mammary tumors at early and late stages (Figure 1a). Briefly, metastatic B16 melanoma or MVT1 mammary tumor cells were injected via the tail vein in to syngeneic mice (C57/BL6 and FVB/N backgrounds, respectively). Lungs were harvested 1 and 2 weeks post injection of tumor cells to capture metastases at different stages of growth (Figure 1b). Subsequently, global microRNA profiling of RNA isolated from lung TIMs at the two timepoints was performed. 17 microRNA were seen to be up-regulated at 2 weeks compared to 1 week post injection (>2 fold) in melanoma associated macrophages (Figure 1c; Supplementary Table S1a) whereas the expression of 8 miRs increased (>2 fold) in metastatic mammary tumor TIMs (Figure 1d; Supplementary Table S1b). Notably, 5 miRs namely miR-21, miR-29a, miR-142-3p, miR-181a and miR-223 were up-regulated in TIMs from both tumor models (Figure 1e). In contrast, although several miRs were downregulated in tumor TIMs from both melanoma and mammary tumor models, there was no overlap between the two groups.

### The CSF1-ETS2 pathway activates the expression of miR-21, mir-29a, miR-1423p and miR-223 in myeloid cells

To elucidate signaling upstream of the miRs that regulates their expression, we analyzed regulatory regions surrounding the coding loci of the 5 miRs to identify transcription factor binding motifs. Intriguingly, we found conserved ETS motifs proximal to all 5 miR loci. Our group has previously shown that deletion of the transcription factor *Ets2* in macrophages resulted in reduced metastatic tumor burden in three different models of metastasis.<sup>17</sup> To test the hypothesis that ETS2 may regulate these miRs, miR expression was analyzed in mature myeloid cells with deletion of *Ets2*. *Ets2* depletion in TIMs in the MVT1 model resulted in a down-regulation of 4 of the 5 miRs, namely miR-21, miR-29a, miR-142-3p and miR-223 (Figure 2a). We performed standard chromatin immunoprecipitation (ChIP) assays on the four microRNA loci using primers designed around the putative ETS-binding sites. ChIP experiments on bone marrow derived macrophages(BMMs) confirmed that ETS2 is enriched at all four miR loci. Further, binding was ablated when *Ets2* was deleted in macrophages (Figure 2b-e).

ETS2 expression and phosphorylation is mediated via the CSF1-ERK pathway.<sup>18</sup> A highly selective inhibitor of CSF1R kinase activity, GW2580 (ref. 19), was employed to confirm that the miRs were downstream of the CSF1-ETS2 pathway. Mice were treated with GW2580 via oral gavage beginning the 4th day post-injection of metastatic MVT1 cells for 3 consecutive days (days 4-6). Lungs were harvested 7 days post-injection for analysis. In parallel, TIMs were sorted from lungs of the treated mice to determine whether miR expression changes in response to drug treatment. Myeloid cells from the lungs of GW2580

treated mice exhibited lower levels of the four ETS2-responsive miRs (Figure 2f). Concomitantly, GW2580 treatment led to a significant 20% reduction in tumor cell proliferation in the lungs of treated mice compared to controls (Figure 2g). At this stage there was little evidence of tumor angiogenesis in either treatment or control group (data not shown) so mice were sacrificed at later stages to assess blood vessel growth. For these experiments, mice were treated with GW2580 beginning on day 9 for 5 consecutive days (days 9-13). Lungs were harvested on day 14 for histological analysis. The size of blood vessels as well as vessel branching were decreased by GW2580 treatment (Figure 2h) though there was no effect on tumor cell proliferation at this stage (Supplementary Figure S1a). GW2580 treatment didn't alter macrophage infiltration in lung lesions (Supplementary Figure S1b) and treatment of tumor cells with GW2580 didn't affect miR-21 or miR-29a levels (Supplementary Figure S1c).

### **Selective ablation of *Dicer* in myeloid cells results in reduced melanoma and mammary tumor metastasis in mice**

Conditional deletion of the endonuclease *Dicer* was utilized to assess the functional consequence of miR depletion on metastasis. *Lys-cre*, which is active only in mature myeloid cells and macrophages<sup>20</sup>, was utilized to achieve specific deletion of *Dicer* and a simultaneous reduction of all four miRs (Supplementary Figure S2a,b,c). TIMs were sorted from metastatic lungs 2 weeks post injection of B16 melanoma cells from mice with conditional knockout of *Dicer* (*Dicer* KO) and wild-type controls. The expression of miR-21, miR-29a, miR-142-3p and miR-223 were all seen to decrease in *Dicer* KO TIMs (Supplementary Figure S2d). To determine if ablation of miR expression in macrophages affects metastasis, wild-type and experimental mice were injected with either B16 melanoma cells or the EO771 metastatic mammary tumor cell line. C57/B16 EO771 cells were used since the *Dicer* KO mice were on a C57/B16 background. Lungs were harvested 2 weeks post injection for histology. *Dicer* KO mice exhibited considerably less metastatic tumor burden when compared to wild-type controls in both the metastatic melanoma (Figure 3a) and mammary tumor models (Figure 3d). Immunofluorescent staining revealed that there was a reduction in tumor cell proliferation in the metastatic melanoma (Figure 3b) and mammary tumor (Figure 3e) lung lesions in the *Dicer* KO mice relative to controls. This was accompanied by a decrease in angiogenesis in the melanoma (Figure 3c) and mammary tumor (Figure 3f) models. There was no difference in macrophage infiltration in metastatic tumors between the genotypes (Supplementary Figure S2e).

### **Modulation of miR-21 and miR-29a levels in macrophages affects tumor cell proliferation and angiogenesis**

To test whether the miRs function in a non-cell autonomous manner to promote metastatic tumor growth, matrigel plug assays were used to study the effect of overexpression and knockdown of individual miRs in macrophages (see Materials and Methods). There was no difference in macrophage numbers in plugs with miR-21, miR-29a over-expressing macrophages when compared to the scrambled control (Supplementary Figure S3a). Over-expression of miR-21 and miR-29a in macrophages caused increased growth of blood vessels into the matrigel plugs as revealed by CD31 staining whereas knockdown of miR-21 resulted in reduced angiogenesis (Figure 4a,c). Knockdown of mir-29a didn't have a

significant effect on angiogenesis which might be due to redundancy between miR-29a and other miR-29 family members, including miR-29b and miR-29c. miR-21 and miR-29a overexpression in macrophages also promoted tumor cell proliferation in the plug assay while knockdown of the miRs led to a significant reduction in proliferation (Figure 4b,d). Exogenous miR-21 and miR-29a expression in macrophages co-cultured with MVT1 cells *in vitro* increased tumor cell proliferation (Figure 4e). Co-transfection of both miR-21 and miR-29a in macrophages didn't appear to significantly affect angiogenesis and tumor cell proliferation compared to individual miRs (Figure 4a,b,e). miR-142-3p and miR-223 overexpression also led to increased angiogenesis but had no discernable effect on tumor cell proliferation (Supplementary Figure S3b). Similar results were obtained upon miR-21, miR-29a and miR-223 over-expression in macrophages in a melanoma matrigel model (Supplementary Figure S3c,d).

### **miR-21 and miR-29a target anti-angiogenic modulators and genes involved in M1 polarization**

Expression of putative mRNA targets of the onco-miRs, identified *in silico*, along with genes important for M2 polarization<sup>17,18,21,22,23</sup>, was analyzed using the nanostring platform. Intriguingly, 13 miR-29a target genes have previously been reported to be regulated by ETS2 (Supplementary Table S2) (ref.17). TIMs were sorted from lungs 2 days, 1 week and 2 weeks post MVT1 injection and subjected to expression profiling. A striking negative correlation between miR-21 and miR-29 levels and the expression of putative target genes (marked by red asterisks in Figure 5a, Supplementary Table S2) was observed. In particular, there was decreased expression of genes associated with M1 polarization, like *Fas* and *Il12a* (Figure 5a). This was accompanied by upregulation of M2-like genes, such as *Arg1* and *Cd204* in macrometastases associated TIMs (Figure 5a). Similarly, the expression of a cadre of genes associated with the negative regulation of angiogenesis was seen to decrease, while positive regulators *Hif1a* and *Vegfa* increased (Figure 5a). A subset of these anti-tumor targets were confirmed via ectopic expression of these miRs in BMMs, which led to reduced mRNA levels of the miR-21 targets *Pdcd4*, *Spry1* and *Timp3* (Figure 5b) and the miR-29a targets *Col4a2*, *Sparc* and *Timp3* (Figure 5d). Further, protein levels of miR targets were also seen to decrease in these assays (Figure 5c,e). Conversely, immunofluorescent staining revealed that knockdown of the miRs results in increased expression of the common target TIMP3 *in vivo* (Figure 5f). The anti-angiogenic genes *Col4a2*, *Fbn1* and *Sparc* were also confirmed to be miR-29 targets through reporter luciferase assays (Supplementary Figure S3e).

### **Myeloid cells in human brain metastases exhibit active CSF1 signaling accompanied by miR-21 and miR-29a expression**

To assess the relevance of the miRs identified in our mouse models to human metastatic cancer, human brain metastatic breast cancer samples were analyzed. Immunostaining for the activated form of the CSF1R, CSF1R-pY723 and the macrophage/microglia marker IBA1, was performed on nine independent patient samples to test whether the CSF1/CSF1R pathway is active in human metastatic disease (Figure 6a). We observed that CSF1R-pY723 could be detected in 25-45% IBA1+ cells in all nine human samples tested (Figure 6a). Further, double staining of these samples using a CSF1R antibody recognizing all forms of

the receptor in combination with anti-Keratin8 demonstrated that tumor cells did not express CSF1R (Supplementary Figure S4a).

Because earlier studies had revealed that miR-21 and miR-29a are up-regulated in invasive breast cancer, we selected them for further analysis in the brain metastatic tumors.<sup>24,25</sup> The expression of miR-21 and miR-29a in CSF1R+ cells was determined by performing double microRNA/mRNA *in situ* hybridization in combination with *Csf1r* mRNA (Figure 6b,c,d). The experiments demonstrated that on average 50% of *Csf1r* mRNA positive cells also expressed miR-21 (Figure 6c, Supplementary Figure S4b) and ~75% co-localized with miR-29a expression (Figure 6d, Supplementary Figure S4c). While miR-21 expression was limited to cells that co-express *Csf1r* mRNA, miR-29a was found to be highly expressed in other cells, primarily in tumor cells based on nuclear morphology.

In parallel studies, the co-expression of *Csf1r* mRNA and miR-29a was studied on a separate cohort of patient samples for which lymph node metastases and matched primary tumors were available. Due to limiting amounts of tissue, expression of miR-29a alone could be analyzed (Figure 6e, Supplementary Figure S4d). We observed that the number of *Csf1r* mRNA+ cells infiltrating lymph node metastases was higher than in the primary tumor (Figure 6f). In addition, there was a striking increase in miR-29a levels in *Csf1r*+ cells in lymph node metastases when compared to matched primary tumors (Figure 6g).

### **Expression of miR-21 and miR-29a in CD115<sup>+</sup>CD14<sup>lo</sup>CD16<sup>hi</sup> myeloid cells derived from the blood of patients correlates with metastatic tumor burden**

Tumors exert a systemic effect on myeloid cells that is critical for colonization and growth of metastases.<sup>26,27</sup> Consistent with previous work, tumor growth in the lungs of mice injected with MVT1 cells correlated with a significant expansion of CD11b+GR1+ myeloid cells in the bone marrow (Figure 7a). The levels of miR-21 and miR-29a increased in this CD11b+GR1+ population (Figure 7b,c).

To determine if a similar expansion occurs in metastatic breast cancer patients, we analyzed the CD115+ (CSF1R+) myeloid population of leukocytes in the blood of patients. An increase in the percentage of CD115+ cells in patients (n=13) compared to normal volunteer controls (n=8) was detected (Figure 7d). Further analysis of the CD115+ population demonstrated that a CD14<sup>lo</sup>CD16<sup>hi</sup> non-classical monocyte population<sup>28</sup> was significantly expanded in the metastatic cancer patients, while the CD14<sup>hi</sup>CD16<sup>lo</sup> classical monocyte population was depleted (Figure 7e).

The CD115<sup>hi</sup>CD14<sup>lo</sup>CD16<sup>hi</sup> population was collected and the expression of miR-21 and miR-29a was determined. For this analysis, the patient samples were classified as “low” or “high” metastatic burden based on bone scans or PET scans revealing visceral metastasis, especially for the high group (Figure 7f, Supplementary Figure S5a,b). The expression of both miR-21 and miR-29a were significantly up-regulated in the CD115<sup>hi</sup>CD14<sup>lo</sup>CD16<sup>hi</sup> population in patients with high metastatic tumor burden in visceral organs when compared to patients with limited metastasis (Figure 7g).

## DISCUSSION

Research over the past decade has established the role of TIMs in promoting multiple steps in the metastatic cascade.<sup>4</sup> The present work focused on the function of mature myeloid cells during the last stage of metastatic disease progression, the growth of tumors at the distant organ site. These studies demonstrate that miR-21 and miR-29a expression is activated in TIMs in mouse models of metastasis, promoting tumor angiogenesis and tumor cell proliferation. Notably, the two oncomiRs are robustly expressed in CSF1R-positive macrophages located in human breast cancer brain and lymph node metastases, while expression is lower in primary tumors. Taken in sum, these experiments reveal a novel CSF1-ETS2-miR pathway in myeloid cells that controls the proliferation and growth of metastatic tumors. However, the myeloid cell markers employed in this study, namely F4/80 and Csf1r-YFP, are expressed on various myeloid sub-classes present in the metastatic microenvironment, including inflammatory monocytes<sup>7</sup>, F4/80+ myeloid derived suppressor cells<sup>29</sup> and Tie2 expressing monocytes<sup>30</sup>. Further studies are required to delineate the exact identity of the miR-expressing cells contributing to angiogenesis and tumor growth.

The results presented provide new insights into post-transcriptional regulatory mechanisms in metastatic TIMs. Reports on microRNA dysregulation in TIMs so far have mostly focused on tumor suppressor miRs such as miR-155 and miR-511 in primary tumors.<sup>15,16</sup> Interestingly, the expression of both these miRs didn't change significantly in metastatic melanoma and mammary tumor derived TIMs, suggesting that unique post-transcriptional mechanisms may operate at metastatic sites. Our studies revealed that global depletion of miRs impeded metastatic tumor growth and angiogenesis in mouse models of melanoma as well as breast cancer. In addition, knockdown of either miR-21 or miR-29a in macrophages led to reduced tumor cell proliferation. These results suggest that the oncogenic effects of miRs in TIMs are dominant over tumor suppressive effects.

Our studies identified targets downstream of the miRs that enable their pro-tumor function. A negative correlation between the expression of miR-21/miR-29a and key M1 polarizing molecules in metastatic TIMs including IL-12, IL-23 IFN- $\gamma$ , PDCD4 and TNF- $\alpha$  was observed. Consistent with this data, reports implicate these miRs in inhibiting M1/Th1 type inflammation while promoting M2/Th2 polarization through regulation of these target genes.<sup>31,32,33,34,35</sup> A cohort of genes involved in repressing angiogenesis are also targets of the oncomiRs, including the miR21 target *Timp3* (ref. 36, 37) and miR-29a targets such as *Col4a2* and *Col18a1* (ref. 38). The data suggests that miR-21 and miR-29a promote an 'M2'-like, pro-angiogenic phenotype in tumor associated myeloid cells through their repression of anti-angiogenic and 'M1' genes. Importantly, miR-21 and miR-29a overexpression in macrophages either *in vivo* or *in vitro* promoted tumor cell proliferation, consistent with the acquisition of a pro-tumor M2 phenotype.<sup>39,40</sup> However, co-transfection of miR-21 and miR-29a didn't appear to have a synergistic effect, suggesting that the downstream targets common to both miRs may be the ones that are critical for the miR's pro-tumor functions. One such target may be the MMP inhibitor TIMP3, whose expression was seen to increase when either miR-21 or miR-29 were knocked down. The combined effect of these miRs in promoting angiogenesis and thwarting anti-tumor immune responses may act as a catalyst for micro-metastases to proliferate at the metastatic site. A recent study

demonstrates that tumor cell secreted miR-21 and miR-29a activate pro-tumor functions in myeloid cells.<sup>41</sup> In addition, macrophages are also known to release microRNA through microvesicles<sup>42</sup> and miR-21 acts as an oncogene even within tumor cells.<sup>43,44</sup> Conceivably, these miRs in TIMs may function both in an autocrine and paracrine fashion to remodel the metastatic tumor microenvironment.

Our results also highlight the synergy between CSF1 driven transcriptional and post-transcriptional gene regulation in tumor associated myeloid cells. ETS2, a well-defined nuclear effector of CSF1/MAPK signaling, functions to modulate expression of several of the identified miRs. Further, ETS2 represses anti-angiogenic targets, for example TIMP3, at both the transcriptional level<sup>17</sup>, and indirectly at the post-transcriptional level through miR-21 and miR-29a. The coupling of gene regulatory mechanisms by ETS2 may allow for a more rapid and complete response to CSF1 locally and systemically. From a therapeutic standpoint, our work underscores the potential utility of targeting CSF1-ETS2 signaling along with tumor-targeted therapies at metastatic sites. Inhibiting CSF1 signaling not only altered miR expression in myeloid cells, but also affected tumor cell proliferation and angiogenesis. Inhibition of the signaling upstream of the miRs might also be more beneficial than targeting the miRs themselves as some reports ascribe a tumor suppressive role for miR-29 in epithelial cells<sup>45</sup> and Dicer acts as a haploinsufficient tumor suppressor in certain tumors.<sup>46</sup> Recent studies in preclinical models of breast cancer, melanoma and glioma provide evidence for the efficacy of targeting tumor macrophages using CSF1R inhibitors to improve therapies directed at primary tumors.<sup>47,48,49,50</sup> Our findings suggest that targeting CSF1 signaling may also be effective in the treatment of metastatic tumors that cause the majority of patient mortality in breast cancer and melanoma.

Another intriguing observation from our studies was the systemic expansion of myeloid populations in both our mouse models and human metastatic breast cancer. The activation of miR-21 and miR-29a expression occurs both in CD11b+GR1+ cells in the bone marrow of metastatic tumor bearing mice and CD115+ non-classical monocytes from patients, and inhibition of the CSF1 signaling pathway in mouse models resulted in decreased miR-21 and miR-29a levels in TIMs. Therefore, the expression of the CSF1-dependent miRs could potentially be utilized as a correlative biomarker for therapeutic efficacy in patients being treated with CSF1 signaling inhibitors currently in Phase I clinical trials for the treatment of solid tumors.

Collectively, our findings provide key insights into the pro-tumor function of microRNA in metastatic tumor associated myeloid cells. We delineate a CSF1-ETS2 activated miR signature in the metastatic tumor microenvironment that mediates cross-talk between epithelial cells and macrophages and accelerates metastatic tumor progression via multiple mechanisms. It remains to be seen whether a similar microRNA signature exists in the case of other metastatic solid cancers. In addition, identification of other signaling pathways that synergize with CSF1 signaling in the metastatic tumor microenvironment will be vital for the development of effective therapies to combat metastatic disease.

## MATERIALS AND METHODS

### Mice

The *Ets2<sup>LoxP</sup>* allele, *Ets2<sup>db</sup>* knockout allele, and *Lys-Cre* knockin allele have been previously described.<sup>20,51,52</sup> The *c-fms-YFP* (Csf1r-YFP) construct has been described previously.<sup>17</sup> All these alleles were bred >10 generations into the FVB/N background. The *Dicer<sup>LoxP</sup>* and a separate *Lys-Cre* on a C57Bl/6 background were obtained from Jackson Laboratories (Bar Harbor, ME, USA). All mice were taken care of according to the guidelines provided by the Ohio State University Institutional Animal Care and Use Committee.

### Cell culture and transfections

The metastatic mammary tumor cell lines MVT1 and E0771 have been described previously.<sup>53,54</sup> The B16 melanoma cell line<sup>55</sup> was used for experimental melanoma metastasis and matrigel assays. All cell lines were maintained in DMEM containing 10% FBS at 37°C in a 5% CO<sub>2</sub> incubator. To obtain BMMs, bone marrow precursors were flushed out from the femurs and tibiae of 4 week old female FVB/N or C57Bl/6 mice and cultured in 25 ng/ml CSF1 for 4 days in non-tissue culture treated square dishes. BMMs were transfected with 10nM microRNA precursors, anti-miR oligos or scrambled controls using the Amaxa Nucleofector system (Lonza, Walkersville, MD, USA) for the matrigel plug assays and *in vitro* tumor cell-BMM admixture studies.

### Animal procedures

For orthotopic tail vein injections, 7-10 week old female FVB/N or C57Bl/6 mice were placed in a tail vein restrainer device (Braintree Scientific, Braintree, MA, USA). After diluting either lateral vein, a 28 ½ G insulin syringe needle was used to inject 3×10<sup>6</sup> MVT1, 5×10<sup>5</sup> EO771 or B16 melanoma cells re-suspended in 200ul sterile PBS. Mice were harvested 2 days, 1 week and 2 weeks post injection. For subcutaneous matrigel plug injections, 6-10 week old female FVB/N or C57Bl/6 mice were injected in the flank with 350ul of ice cold matrigel containing 2.5 × 10<sup>5</sup> MVT1 or B16 melanoma cells admixed with 2.5 × 10<sup>5</sup> BMMs. Plugs were harvested and embedded in OCT 5 days post injection for histology.

### Isolation of cells from tumor bearing mice

Tumor bearing lungs were minced and digested enzymatically using collagenase type 2 (Worthington, Lakewood, NJ) and DNaseI (Roche Applied Science, Indianapolis, IN, USA) at 37°C with constant shaking. The Csf1r-YFP or F4/80 positive myeloid populations (TIMs) were sorted on the BD FACS Aria/ AriaIII. For bone marrow studies, bone marrow precursors were flushed out from the femurs and tibiae of metastatic tumor bearing mice and myeloid cells were sorted using PE conjugated anti-CD11b (BD Pharmingen, San Jose, CA, USA) and APC conjugated anti-GR1 antibodies (eBioscience, San Diego, CA, USA).

### ***In vivo* Inhibitor studies using GW2580**

For *in vivo* studies, GW2580 (LC Labs, Woburn, MA, USA) was suspended in a 0.5% hydroxypropylmethylcellulose and 0.05% Tween-80 solution. Animals were gavaged with 160mg/kg GW2580 daily until they were sacrificed.<sup>48</sup>

### **Expression profiling using nCounter technology**

RNA isolation from TRIzol (Invitrogen, Carlsbad, CA) was performed according to manufacturer's instructions. A custom nCounter mRNA gene expression codeset (Nanostring Technologies, Seattle, WA, USA) (Supplementary TableS2) was built to analyze expression of miR target genes and genes relevant to pro-tumor processes in TIMs. Data was normalized to the geometric mean of the top 50 expressors. For microRNA analysis, the nCounter mouse miRNA expression assay from Nanostring Technologies was used. Data was normalized using the geometric mean of top 100 expressors. The nCounter microRNA assay was used to determine the counts of microRNA in Dicer WT and Dicer KO TIMs. For all experiments, negative control counts were used to set the background for expression of the miRs. Since *Dicer* deletion results in a global depletion of microRNA, technical normalization relative to positive control RNA counts was utilized.

### **Immunostaining**

Tissue and matrigel plugs were either frozen or fixed in formalin and paraffin embedded. 5  $\mu$ m sections were prepared for immunostaining. The following primary antibodies were utilized: rat  $\alpha$ -mouse F4/80 (1:100; Invitrogen), rat  $\alpha$ -mouse CD31 (1:50; BD Biosciences), rabbit  $\alpha$ -mouse Ki67 (1:100; Abcam, Cambridge, MA, USA), rat  $\alpha$ -mouse KERATIN8 (1:400; TROMA-I, Iowa City, IA, USA), rat  $\alpha$ -mouse MECA32 (1:100; TROMA-I), rabbit  $\alpha$ -human CSF1R (1:100; Abcam), goat  $\alpha$ -human IBA1 (1:100; Abcam), rabbit  $\alpha$ -TIMP3 (1:100; Abcam) and rabbit  $\alpha$ -human p-CSF1R(Y723) (1:100 dilution with biotin-streptavidin amplification; Cell Signaling, Beverly, MA, USA). Alexa fluor 488 and 594 conjugated secondary donkey  $\alpha$ -rat, goat  $\alpha$ -mouse, or donkey  $\alpha$ -rabbit antibodies (1:250; Invitrogen) were used for fluorescent detection. Images were acquired using a Nikon Eclipse E800 microscope equipped with a Photometrics Coolsnap camera. MetaVue software (Molecular Devices, Sunnyvale, CA, USA) was used for image acquisition. Confocal microscopy was done on an Olympus FV1000 Filter Confocal system.

Immunohistochemical staining was imaged using a Nikon Eclipse 50i microscope equipped with an AxioCam HRC camera (Zeiss, Thornwood, NY, USA). All images were acquired at room temperature. Immunohistochemical data was quantified by calculating the area of antibody staining per unit area of tumor using FIJI software.<sup>56</sup> Blood vessel size was computed using the connected region plugin in the FIJI software.

### **Western Blot Analysis**

Western blot analysis was performed using lysates from transfected macrophages. The primary antibodies used were goat  $\alpha$ -mouse SPRY1 (1:500; Santa Cruz, Dallas, TX, USA), rabbit  $\alpha$ -human PDCD4 (1:1000; Abcam), rabbit anti-mouse ADAMTS5 (1:500; Santa Cruz) and goat  $\alpha$ -mouse SPARC (1:500; R&D systems, Minneapolis, MN, USA). HRP-linked secondary antibodies were employed.

### **In situ hybridization for CSF1R mRNA and miR-29 on human tumor tissue**

Use of human tissue was approved by the Ohio State University Institutional Review Board (IRB). In situ hybridization was performed using QuantiGene ViewRNA miRNA and mRNA probes (Panomics, Santa Clara, CA, USA). A protocol developed by the Solid Tumor Translational Core at the Ohio State University was used to perform double in situ hybridization for *Csf1r* mRNA and either miR-21 or miR-29a. Imaging was done on the Olympus FV1000 Filter Confocal system using a UPLFLN 40x oil objective (N.A. 1.3). Consecutive sections stained with a scrambled probe were utilized to set the background threshold for image acquisition. The Cy3 channel was employed to detect fluorescence miR-21 and miR-29a signal whereas the Cy5 channel was used to detect *Csf1r* mRNA hybridization signal.

### **Chromatin immunoprecipitation assays**

Chromatin immunoprecipitation (ChIP) assays were performed on BMMs with 20ug of anti-ETS2 as described previously.<sup>51,57</sup> Rabbit-IgG was used as a control (Millipore, Billerica, MA, USA). Samples were analyzed by real-time PCR using the Roche Universal Probe Library (Roche Applied Science) and the Universal Master mix (Applied biosystems, Grand Island, NY, USA).

### **Sorting and analysis of CD115+ populations from patient blood**

RBCs were removed by osmotic lysis and viable white blood cells were stained with fluorophore conjugated antibodies for the markers of interest. Cells were sorted based on the co-expression of CD115 and CD45, and further analyzed for CD14 and CD16 positivity. The following antibodies were used:  $\alpha$ -CD45(PE/Cy7)(BDPharmingen),  $\alpha$ -CD115(PE),  $\alpha$ -CD14(APC/Cy7) and  $\alpha$ -CD16(AF700) (Biolegend, San Diego, CA, USA). RNA from CD115+CD16+ cells was used for miR real time PCR analysis.

### **Quantitative real time PCR**

For mRNA targets of miRs, the Roche Universal Probe Library system was used. For miR-21 and -29a qRT-PCR, Taqman probes (Applied Biosystems) were utilized. U6 snRNA and snoRNA 202 were used as a housekeeping controls. The Applied Biosystems StepOne Plus instrument was used. Relative expression of the miRs compared to U6 snRNA or snoRNA202 was computed using a variation of the ddCt method.<sup>58</sup>

### **Statistical analysis**

Minitab, GraphPad and Excel were used for statistical analysis. For analysis of all data, an unpaired Student's *t* test was used unless otherwise stated. All error bars depict SEM.

### **Supplementary Material**

Refer to Web version on PubMed Central for supplementary material.

## ACKNOWLEDGEMENTS

We thank Yongqi Wu for help with flow cytometry. We also wish to acknowledge the histology core, OSU Comprehensive Cancer Center Microarray, Nucleic Acids, Analytical Cytometry, Microscopy and Biostatistics Core Shared Resources for technical assistance. This work was funded through National Institutes of Health grants (NIHPO1CA097189, RO1CA053271) and the Evelyn Simmers Foundation to M.C.O.

## REFERENCES

1. Bröcker EB, Zwadlo G, Suter L, Brune M, Sorg C. Infiltration of primary and metastatic melanomas with macrophages of the 25F9-positive phenotype. *Cancer Immunol Immunother.* 1987; 25:81–86. [PubMed: 3664532]
2. Leek RD, Harris AL. Tumor-associated macrophages in breast cancer. *J Mammary Gland Biol Neoplasia.* 2002; 7:177–189. [PubMed: 12463738]
3. Jensen TO, Schmidt H, Møller HJ, Høyer M, Maniecki MB, Sjoegren P, et al. Macrophage markers in serum and tumor have prognostic impact in American Joint Committee on Cancer stage I/II melanoma. *J Clin Oncol.* 2009; 27:3330–3337. [PubMed: 19528371]
4. Qian BZ, Pollard JW. Macrophage diversity enhances tumor progression and metastasis. *Cell.* 2010; 141:39–51. [PubMed: 20371344]
5. Chen Q, Zhang XH, Massague J. Macrophage binding to receptor VCAM-1 transmits survival signals in breast cancer cells that invade the lungs. *Cancer Cell.* 2011; 20:538–549. [PubMed: 22014578]
6. Qian B, Deng Y, Im JH, Muschel RJ, Zou Y, Li J, et al. A distinct macrophage population mediates metastatic breast cancer cell extravasation, establishment and growth. *PLoS One.* 2009; 4:e6562. [PubMed: 19668347]
7. Qian BZ, Li J, Zhang H, Kitamura T, Zhang J, Campion LR, et al. CCL2 recruits inflammatory monocytes to facilitate breast-tumour metastasis. *Nature.* 2011; 475:222–225. [PubMed: 21654748]
8. Yan HH, Pickup M, Pang Y, Gorska AE, Li Z, Chytil A, et al. Gr-1+CD11b+ myeloid cells tip the balance of immune protection to tumor promotion in the premetastatic lung. *Cancer Res.* 2010; 70:6139–49. [PubMed: 20631080]
9. Wang T, Ge Y, Xiao M, Lopez-Coral A, Azuma R, Somasundaram R, et al. Melanoma-derived conditioned media efficiently induce the differentiation of monocytes to macrophages that display a highly invasive gene signature. *Pigment Cell Melanoma Res.* 2012; 4:493–505. [PubMed: 22498258]
10. Chen P, Huang Y, Bong R, Ding Y, Song N, Wang X, et al. Tumor-associated macrophages promote angiogenesis and melanoma growth via adrenomedullin in a paracrine and autocrine manner. *Clin Cancer Res.* 2011; 17:7230–7239. [PubMed: 21994414]
11. Zaidi MR, Davis S, Noonan FP, Graff-Cherry C, Hawley TS, Walker RL, et al. Interferon- $\gamma$  links ultraviolet radiation to melanomagenesis in mice. *Nature.* 2011; 469:548–553. [PubMed: 21248750]
12. Esquela-Kerscher A, Slack FJ. Oncomirs - microRNAs with a role in cancer. *Nat Rev Cancer.* 2006; 6:259–69. [PubMed: 16557279]
13. O'Connell RM, Rao DS, Chaudhuri AA, Baltimore D. Physiological and pathological roles for microRNAs in the immune system. *Nat Rev Immunol.* 2010; 10:111–122. [PubMed: 20098459]
14. Liu G, Abraham E. MicroRNAs in immune response and macrophage polarization. *Arterioscler Thromb Vasc Biol.* 2013; 33:170–177. [PubMed: 23325473]
15. Squadrito ML, Pucci F, Magri L, Moi D, Gilfillan GD, Ranghetti A, et al. miR-511-3p modulates genetic programs of tumor-associated macrophages. *Cell Rep.* 2012; 1:141–154. [PubMed: 22832163]
16. Zonari E, Pucci F, Saini M, Mazzieri R, Politi LS, Gentner B, et al. A role for miR-155 in enabling tumor-infiltrating innate immune cells to mount effective anti-tumor responses. *Blood.* 2013; 122:243–52. [PubMed: 23487026]

17. Zabuwala T, Taffany DA, Sharma SM, Merchant A, Adair B, Srinivasan R, et al. An ets2-driven transcriptional program in tumor-associated macrophages promotes tumor metastasis. *Cancer Res.* 2010; 70:1323–1333. [PubMed: 20145133]
18. Fowles LF, Martin ML, Nelsen L, Stacey KJ, Redd D, Clark YM, et al. Persistent activation of mitogen-activated protein kinases p42 and p44 and ets-2 phosphorylation in response to colony-stimulating factor 1/c-fms signaling. *Mol Cell Biol.* 1998; 18:5148–5156. [PubMed: 9710599]
19. Conway JG, McDonald B, Parham J, Keith B, Rusnak DW, Shaw E, et al. Inhibition of colony-stimulating-factor-1 signaling in vivo with the orally bioavailable cFMS kinase inhibitor GW2580. *Proc Natl Acad Sci U S A.* 2005; 102:16078–83. [PubMed: 16249345]
20. Clausen BE, Burkhardt C, Reith W, Renkawitz R, Forster I. Conditional gene targeting in macrophages and granulocytes using LysMcre mice. *Transgenic Res.* 1999; 8:265–277. [PubMed: 10621974]
21. Rae F, Woods K, Sasmono T, Campanale N, Taylor D, Ovchinnikov DA, et al. Characterisation and trophic functions of murine embryonic macrophages based upon the use of a Csf1r-EGFP transgene reporter. *Dev Biol.* 2007; 308:232–46. [PubMed: 17597598]
22. Tagliani E, Shi C, Nancy P, Tay CS, Pamer EG, Erlebacher A. Coordinate regulation of tissue macrophage and dendritic cell population dynamics by CSF-1. *J Exp Med.* 2011; 208:1901–1916. [PubMed: 21825019]
23. Mossadegh-Keller N, Sarrazin S, Kandalla PK, Espinosa L, Stanley ER, Nutt S, et al. M-CSF instructs myeloid lineage fate in single haematopoietic stem cells. *Nature.* 2013; 497:239–243. [PubMed: 23575636]
24. Yan LX, Huang XF, Shao Q, Huang MY, Deng L, Wu QL, et al. MicroRNA miR-21 overexpression in human breast cancer is associated with advanced clinical stage, lymph node metastasis and patient poor prognosis. *RNA.* 2008; 14:2348–2360. [PubMed: 18812439]
25. Gebeshuber CA, Zatloukal K, Martinez J. miR-29a suppresses tristetraproline, which is a regulator of epithelial polarity and metastasis. *EMBO rep.* 2009; 10:400–405. [PubMed: 19247375]
26. Gao D, Mittal V. The role of bone-marrow-derived cells in tumor growth, metastasis initiation and progression. *Trends Mol Med.* 2009; 15:333–343. [PubMed: 19665928]
27. Gabrilovich DI, Ostrand-Rosenberg S, Bronte V. Coordinated regulation of myeloid cells by tumours. *Nat Rev Immunol.* 2012; 22:253–268. [PubMed: 22437938]
28. Strauss-Ayali D, Conrad SM, Mosser DM. Monocyte subpopulations and their differentiation patterns during infection. *J Leukoc Biol.* 2007; 82:244–252. [PubMed: 17475785]
29. Sica A, Bronte V. Altered macrophage differentiation and immune dysfunction in tumor development. *J Clin Invest.* 2007; 117:1155–1166. [PubMed: 17476345]
30. De Palma M, Venneri MA, Galli R, Sergi L, Politi LS, Sampaolesi M, et al. Tie2 identifies a hematopoietic lineage of proangiogenic monocytes required for tumor vessel formation and a mesenchymal population of pericyte progenitors. *Cancer Cell.* 2005; 8:211–226. [PubMed: 16169466]
31. Lu TX, Hartner J, Lim EJ, Fabry V, Mingler MK, Cole ET, et al. MicroRNA-21 limits in vivo immune response-mediated activation of the IL-12/IFN-gamma pathway, Th1 polarization, and the severity of delayed-type hypersensitivity. *J Immunol.* 2011; 187:3362–3373. [PubMed: 21849676]
32. Ma F, Xu S, Liu X, Zhang Q, Xu X, Liu M, et al. The microRNA miR-29 controls innate and adaptive immune responses to intracellular bacterial infection by targeting interferon-gamma. *Nat Immunol.* 2011; 12:861–869. [PubMed: 21785411]
33. Sheedy FJ, Palsson-McDermott E, Hennessy EJ, Martin C, O’Leary JJ, Ruan Q, et al. Negative regulation of TLR4 via targeting of the proinflammatory tumor suppressor PDCD4 by the microRNA miR-21. *Nat Immunol.* 2010; 11:141–147. [PubMed: 19946272]
34. Sica A, Mantovani A. Macrophage plasticity and polarization: in vivo veritas. *J Clin Invest.* 2012; 122:787–795. [PubMed: 22378047]
35. Brain O, Owens BM, Pichulik T, Allan P, Khatamzas E, Leslie A, et al. The intracellular sensor NOD2 induces microRNA-29 expression in human dendritic cells to limit IL-23 release. *Immunity.* 2013; 39:521–536. [PubMed: 24054330]

36. Qi JH, Ebrahem Q, Moore N, Murphy G, Claesson-Welsh L, Bond M, et al. A novel function for tissue inhibitor of metalloproteinases-3 (TIMP3): inhibition of angiogenesis by blockage of VEGF binding to VEGF receptor-2. *Nat Med.* 2003; 9:407–415. [PubMed: 12652295]
37. Gabrieli G, Wurdinger T, Kesari S, Esau CC, Burchard J, Linsley PS, et al. MicroRNA 21 promotes glioma invasion by targeting matrix metalloproteinase regulators. *Mol Cell Biol.* 2008; 28:5369–80. [PubMed: 18591254]
38. Marneros AG, Olsen BR. The role of collagen-derived proteolytic fragments in angiogenesis. *Matrix Biol.* 2001; 20:337–45. [PubMed: 11566268]
39. Lamagna C, Aurrand-Lions M, Imhof BA. Dual role of macrophages in tumor growth and angiogenesis. *J Leukoc Biol.* 2006; 80:705–13. [PubMed: 16864600]
40. Cho HJ, Jung JI, Lim do Y, Kwon GT, Her S, Park JH, et al. Bone marrow-derived, alternatively activated macrophages enhance solid tumor growth and lung metastasis of mammary carcinoma cells in a Balb/C mouse orthotopic model. *Breast Cancer Res.* 2012; 14:R81. [PubMed: 22616919]
41. Fabbri M, Paone A, Calore F, Galli R, Gaudio E, Santhanam R, et al. MicroRNAs bind to Toll-like receptors to induce prometastatic inflammatory response. *Proc Natl Acad Sci U S A.* 2012; 109:E2110–6. [PubMed: 22753494]
42. Yang M, Chen J, Su F, Yu B, Su F, Lin L, et al. Microvesicles secreted by macrophages shuttle invasion-potentiating microRNAs into breast cancer cells. *Mol Cancer.* 2011; 10:117. [PubMed: 21939504]
43. Si ML, Zhu S, Wu H, Lu Z, Wu F, Mo YY. miR-21-mediated tumor growth. *Oncogene.* 2007; 26:2799–803. [PubMed: 17072344]
44. Croce CM. Causes and consequences of microRNA dysregulation in cancer. *Nat Rev Genet.* 2009; 10:704–714. [PubMed: 19763153]
45. Chou J, Lin JH, Brenot A, Kim JW, Provot S, Werb Z. GATA3 suppresses metastasis and modulates the tumour microenvironment by regulating microRNA-29b expression. *Nat Cell Biol.* 2013; 15:201–213. [PubMed: 23354167]
46. Kumar MS, Pester RE, Chen CY, Lane K, Chin C, Lu J, et al. Dicer1 functions as a haploinsufficient tumor suppressor. *Genes Dev.* 2009; 23:2700–2704. [PubMed: 19903759]
47. DeNardo DG, Brennan DJ, Rexhepaj E, Ruffell B, Shiao SL, Madden SF, et al. Leukocyte complexity predicts breast cancer survival and functionally regulates response to chemotherapy. *Cancer Discov.* 2011; 1:54–67. [PubMed: 22039576]
48. Priceman SJ, Sung JL, Shaposhnik Z, Burton JB, Torres-Collado AX, Moughon DL, et al. Targeting distinct tumor-infiltrating myeloid cells by inhibiting CSF-1 receptor: combating tumor evasion of antiangiogenic therapy. *Blood.* 2010; 115:1461–1471. [PubMed: 20008303]
49. Pyonteck SM, Akkari L, Schuhmacher AJ, Bowman RL, Sevenich L, Quail DF, et al. CSF-1R inhibition alters macrophage polarization and blocks glioma progression. *Nat Med.* 2013; 19:1264–72. [PubMed: 24056773]
50. Mok S, Koya RC, Tsui C, Xu J, Robert L, Wu L, et al. Inhibition of CSF1 Receptor Improves the Anti-tumor Efficacy of Adoptive Cell Transfer Immunotherapy. *Cancer Res.* 2014; 74:153–161. [PubMed: 24247719]
51. Wei G, Guo J, Doseff AI, Kusewitt DF, Man AK, Oshima RG, et al. Activated Ets2 is required for persistent inflammatory responses in the motheaten viable model. *J Immunol.* 2004; 173:1374–1379. [PubMed: 15240733]
52. Yamamoto H, Flannery ML, Kupriyanov S, Pearce J, McKercher SR, Henkel GW, et al. Defective trophoblast function in mice with a targeted mutation of Ets2. *Genes Dev.* 1998; 12:1315–26. [PubMed: 9573048]
53. Pei XF, Noble MS, Davoli MA, Rosfjord E, Tilli MT, Furth PA, et al. Explant-cell culture of primary mammary tumors from MMTV-c-Myc transgenic mice. *In Vitro Cell Dev Biol Anim.* 2004; 40:14–21. [PubMed: 15180438]
54. Dunham LJ, Stewart HL. A survey of transplantable and transmissible animal tumors. *J Nat Cancer Inst.* 1953; 13:1299–1377. [PubMed: 13035452]
55. Fidler IJ. Biological behavior of malignant melanoma cells correlated to their survival in vivo. *Cancer Res.* 1975; 35:218–224. [PubMed: 1109790]

56. Schindelin J, Arganda-Carreras I, Frise E, Kaynig V, Longair M, Pietzsch T, et al. Fiji: an open-source platform for biological-image analysis. *Nat Methods*. 2012; 9:676–682. [PubMed: 22743772]
57. Hu R, Sharma SM, Bronisz A, Srinivasan R, Sankar U, Ostrowski MC. Eos, MITF, and PU.1 recruit corepressors to osteoclast-specific genes in committed myeloid progenitors. *Mol Cell Biol*. 2007; 27:4018–4027. [PubMed: 17403896]
58. Livak KJ, Schmittgen TD. Analysis of relative gene expression data using real-time quantitative PCR and the 2<sup>−(Delta Delta C(T))</sup> Method. *Methods*. 2001; 25:402–408. [PubMed: 11846609]

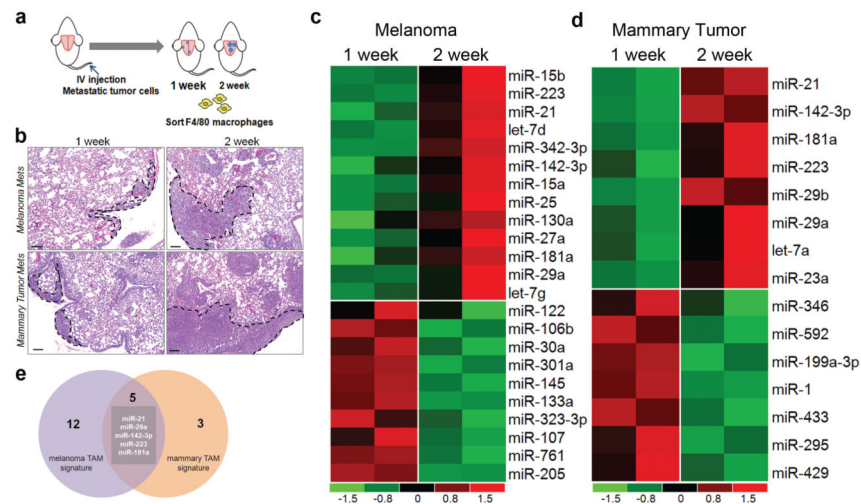


**Figure 1.** Several microRNA are up-regulated in TIMs during metastatic tumor progression. **(a)** Schematic depicting the orthotopic tail vein injection assay **(b)** Representative micrographs showing metastatic lung lesions 1 week and 2 weeks post injection. Scale bar = 100μM. Heatmaps showing that 17 microRNA are upregulated in metastatic melanoma TIMs **(c)** and 8 microRNA are up-regulated in metastatic mammary TIMs **(d)** during metastatic tumor progression. Heatmaps generated using genes > 2 fold change. Profiling data obtained using the nCounter mouse microRNA assay from Nanostring, n=2 mice per group **(e)** Graphic showing miRNAs overlapping between melanoma and mammary tumor profiles.

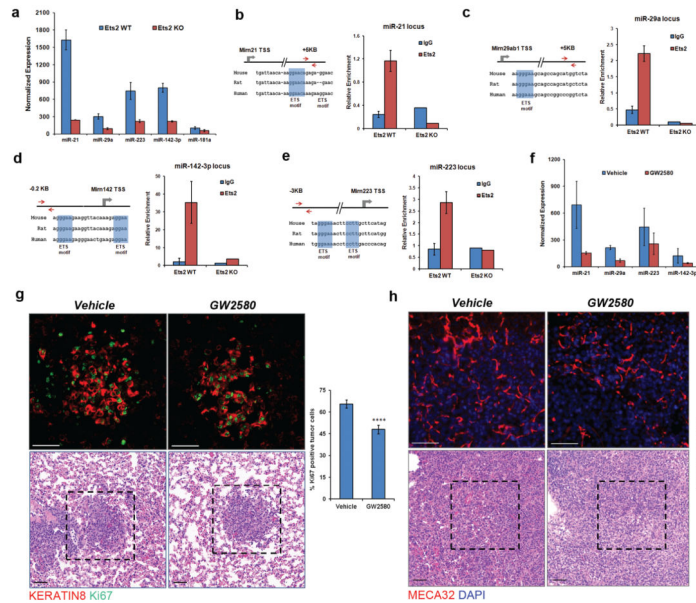


**Figure 2.**

The CSF1-ETS2 pathway regulates the expression of the miRs. **(a)** Bar graph of microRNA expression in *Ets2* WT vs. KO myeloid cells sorted from metastatic lungs. *Ets2*<sup>db/loxP</sup> *lys-cre* mice are denoted as ETS2 KO (n=2 mice per group). ETS2 is enriched at **(b)** the Mirn21 **(c)** Mirn29a **(d)** Mirn142 and **(e)** Mirn223 gene loci in BMMs as determined through ChIP experiments (n= 3 independent samples for miR-21, miR29a and miR-223 promoters for ETS2 WT. n=2 for miR-142 promoter ETS2 WT and n=1 for ETS2 KO for all promoters) **(f)** Bar graph of microRNA expression in lung Csf1r-YFP myeloid cells sorted from GW2580 vs. vehicle treated mice (n=2 per group) **(g)** Double immunofluorescence for epithelial marker Keratin8 (red) and Ki67 (green) in lung lesions (n= 6 GW2580, n=5 vehicle.  $p=6.9 \times 10^{-5}$ . Scale bar= 50uM) **(h)** MECA32 staining in metastatic lung tumors from GW2580 vs. Vehicle treated groups isolated 2 weeks post injection (n=3 per group. \* $p= 0.001$  for vessel size,  $p=0.05$  for branch no. Scale bar= 50uM). Data for all bar graphs represented as mean  $\pm$  SEM.

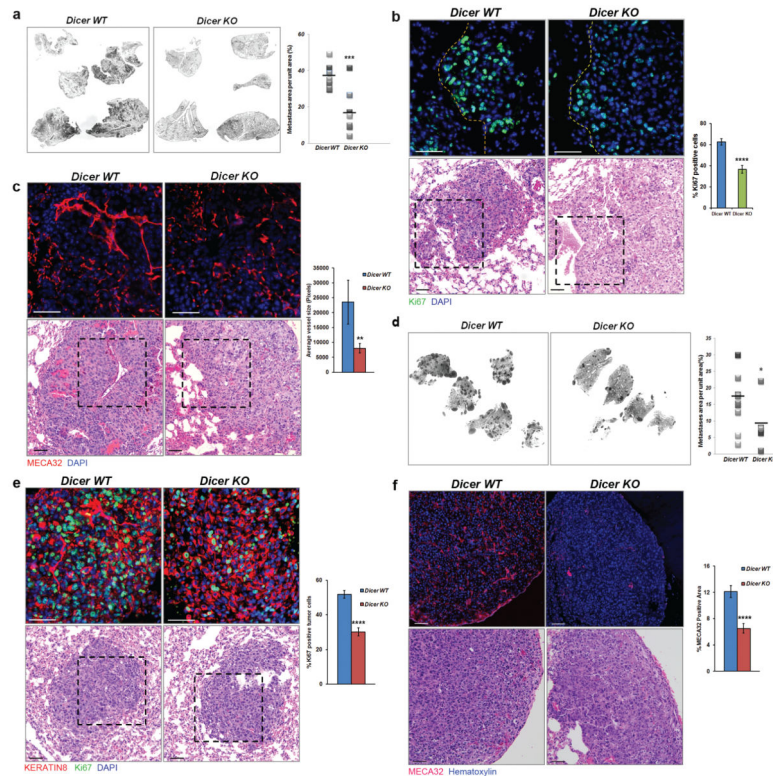


**Figure 3.** Specific deletion of *Dicer* in myeloid cells impedes metastasis. Representative micrographs and quantification of area of metastasis in *Dicer* WT vs. KO mice injected with (a) B16 melanoma cells (n=7 per group, \*p=0.005) and (d) E0771 mammary adenocarcinoma (n=8 *Dicer* WT, n=5 *Dicer* KO, \*p= 0.03). Staining for the proliferation marker Ki67 in metastatic lungs from *Dicer* WT and *Dicer* KO mice in (b) metastatic melanoma (n=4 per group, \*p=1.3 ×10<sup>-6</sup>) and (e) E0771 mammary adenocarcinoma (n=4 per group, \*p=3.7×10<sup>-8</sup>). Representative micrographs and quantification for endothelial marker MECA32 on lungs from *Dicer* WT and *Dicer* KO mice in (c) metastatic melanoma (n=3 *Dicer* WT, n=2 *Dicer* KO, \*p=0.008) and (f) mammary adenocarcinoma (n=6 for *Dicer* WT, n=5 for *Dicer* KO, \*p=0.0002). MECA32 immunohistochemistry on metastatic mammary adenocarcinoma fluorescently pseudocolored after color deconvolution on FIJI software. All scale bars=50uM and all error bars in bar graphs represent SEM.

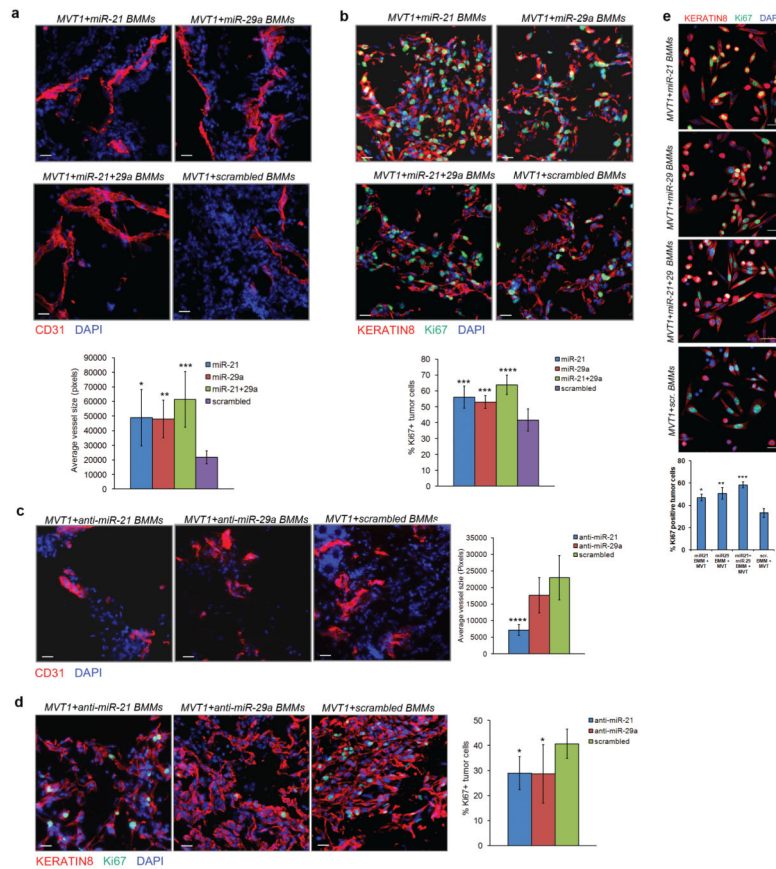


**Figure 4.**

miR-21 and miR-29a regulate pro-tumor processes in myeloid cells. (a) Staining for CD31 in matrigel plugs with miR-21 and miR-29a over expression in macrophages compared to scrambled transfected (n=5 miR-21, n=7 miR-29a, n=5 miR-21+29a, n=8 plugs for scrambled). \*p=0.02 for miR-21; p=0.009 for miR-29a; p=0.001 for miR-21+29a for average vessel size. All comparisons made with respect to the scrambled control) (b) Ki67 Keratin8 double immunostaining in plugs with miR-21, miR-29a, miR-21+29a and scrambled transfected macrophages (\*p=0.001 for miR-21 vs. scrambled; p=0.001 for miR-29a vs. scrambled and p<0.0001 for miR21+29a vs. scrambled. n=4 plugs for miR-21, n=5 miR-29a, n=5 miR21+29a, n=6 scrambled). Scale bar= 20uM (c) Staining for CD31 in matrigel plugs with miR-21 and miR-29a knockdown. n=4 for anti-miR-21, anti-miR-29a and scrambled. \*p=0.0002 for anti-miR-21. All comparisons made with respect to the scrambled control. (d) Ki67 Keratin8 double immunostaining in plugs with miR-21 and miR-29a knockdown in macrophages (n=3 plugs for anti-miR-21, n=4 anti-miR-29a and n=8 scrambled. \*p=0.03 for anti-miR-21 and p=0.03 for anti-miR-29a). Scale bar= 20uM (e) Ki67 Keratin8 double immunofluorescent staining of *in vitro* admixtures of MVT1 cells with miR-21, miR-29a and scrambled transfected macrophages (n=2 per group. \*p<0.05 for miR-21, \*p<0.01 for miR-29a, \*p<0.005 for miR21+29a vs. scrambled). Scale bar = 40uM. P-values calculated using ANOVA with adjustment for pair-wise comparisons.

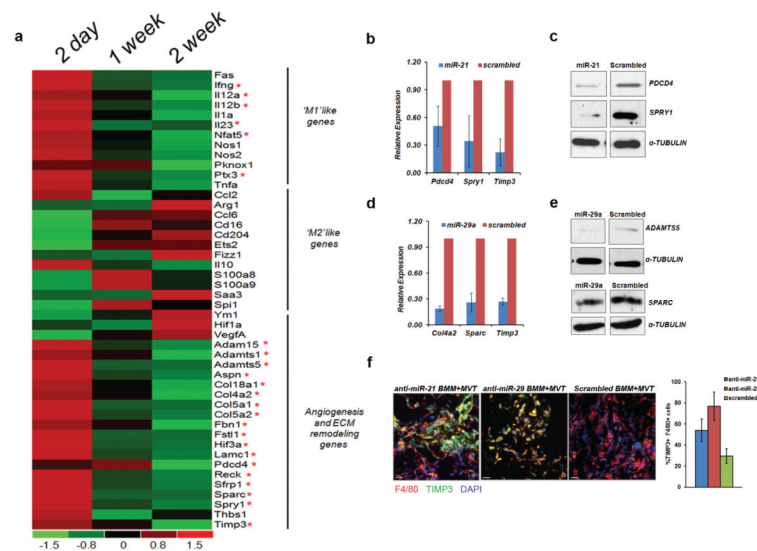


**Figure 5.** miR-21 and miR-29a target anti-angiogenic and M1 polarizing genes. **(a)** Heatmap depicting the changes of expression of key mediators of TIM function in macrophages across the 2 day, 1 week and 2 week timepoints (average of 2 mice per timepoint). There is a negative correlation between the expression of miRs -21 and -29a and the expression of their putative target genes (marked with red asterisks). qRT-PCR for **(b)** miR-21 targets and **(d)** miR-29a targets in BMMs (n=2). Western blot analysis for miR-21 **(c)** and mir-29a targets **(e)**. Representative images for 2 independent experiments **(f)** Immunofluorescent staining for TIMP3 in miR-21 and miR-29a knockdown plugs. n=2 for anti-miR-21, anti-mir-29a and scrambled. Scale bar = 20uM. All bar graphs in this figure depict mean  $\pm$  SEM.

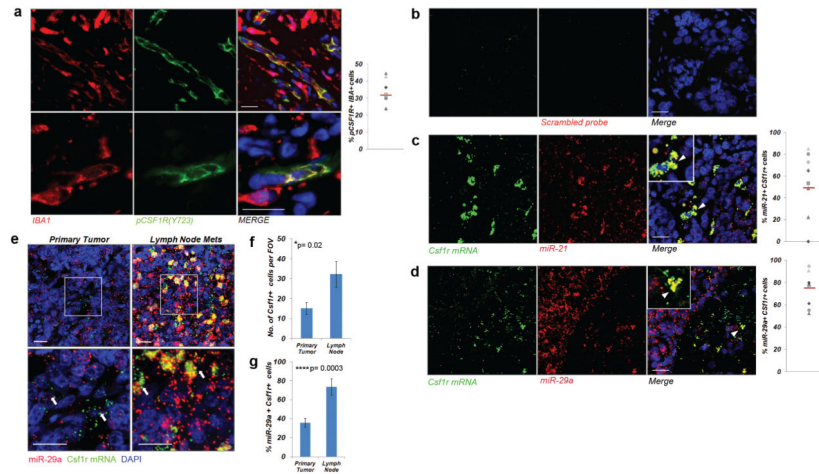


**Figure 6.** miR-21 and miR-29a are expressed in myeloid cells associated with human metastatic breast cancer. **(a)** Staining for myeloid marker IBA1 and pCSF1R(Y723). Mean% IBA1+pCSF1R + cells= 33% **(b)** Representative confocal image of scrambled probe stained sections. Dual in-situ hybridization for **(c)** miR-21(red), **(d)** miR-29a (red) and *Csf1r* mRNA (green). Mean % miR-21+Csf1r+ cells= 55% .Mean % miR-29a+Csf1r+ cells= 74.For **(a),(c),(d)**, dots represent individual values for 9 human brain metastatic breast cancer samples and red bar=mean **(e)** Representative confocal images of miR-29a (red) and *Csf1r* mRNA (green) in-situ hybridization on matched primary tumor and lymph node mets **(f)** Quantification of *Csf1r*+ cells in primary and metastatic tissue (n=5) **(g)** Quantification of miR-29a+*Csf1r*+ double positive cells in primary tumor and lymph node mets (n=5). All data represented as mean  $\pm$  SEM. Scale bars=20uM.

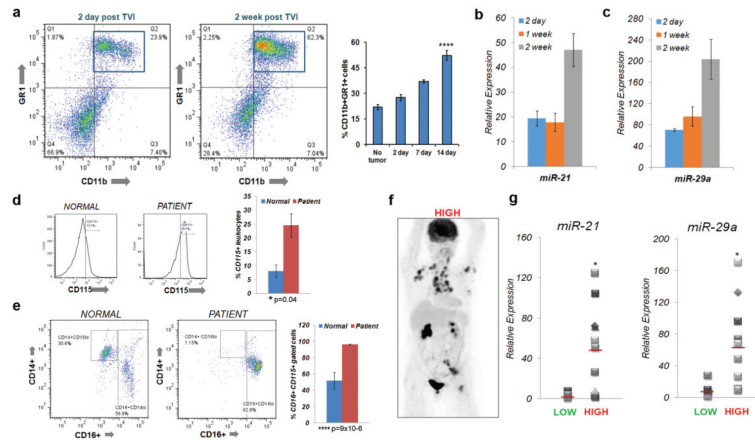


**Figure 7.**

miR-21 and miR-29a are expressed week in myeloid populations in the mouse bone marrow and patient blood during metastatic tumor progression. **(a)** Representative flow plots of CD11b+GR1+ myeloid cells in the bone marrow of mice at 2 days and 2 weeks post injection. Quantification for no tumor, 2 day, 1 week and 2 week timepoints (n=3 mice for no tumor, n=5 for 2 day, n=4 for 1 week, n=6 for 2 week \* $p=3.7 \times 10^{-5}$  for 2 day vs. 2 week comparison). miR-21 **(b)** and miR-29a **(c)** expression in CD11b+GR1+ cells sorted from the bone marrow of mice bearing metastatic tumors in the lung (n=2 mice for 2 day, n=3 mice for 1 week and 2 week post injection). **(d)** Histogram of CD115+ cells from a CD45+ leukocyte gated population in the blood of patients with metastatic breast cancer compared to normal volunteers (n=8 for normal n=13 for patients; \* $p=0.04$  for %CD115+ population increase). **(e)** Flow plots of classical monocyte marker CD14 vs. non-classical monocyte marker CD16 in CD115+ gated cells (n=8 for normal volunteers; n=13 for patients. \* $p=9.0 \times 10^{-6}$  for increase in % CD16 cells in CD115 gated population **(f)** Representative PET scan for patients classified as having ‘high’ metastatic tumor burden. **(g)** miR-21 and **(h)** miR-29a levels in CD115+ CD16+ cells sorted from patients with low vs. high metastatic tumor burden (n=5 for low n=11 for high metastatic burden \* $p=0.01$  for miR-21 and  $p=0.012$  for miR-29a using a two sample t-test at a 95% confidence interval). All bar graphs in this figure depict mean  $\pm$  SEM.